Supporting Information

Halfar et al. 10.1073/pnas.1313775110

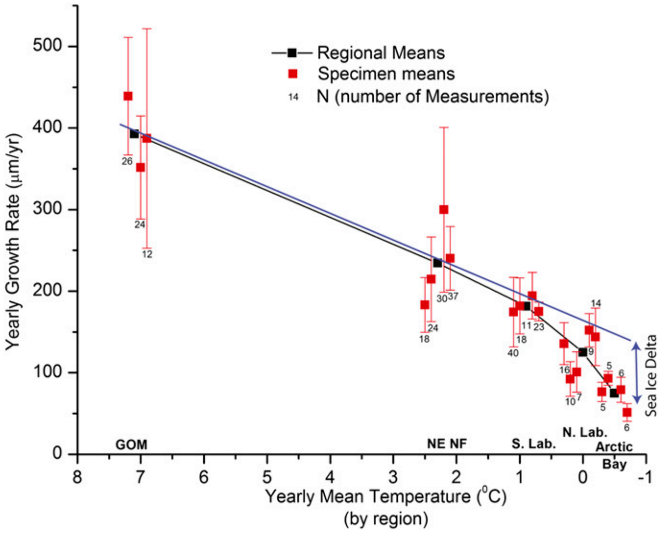

Fig. S1. Annual growth rates across latitudes. Regional yearly growth rates of *Clathromorphum compactum* as a function of sea surface temperature (SST) in the northwestern North Atlantic, Labrador Sea, and Arctic Bay, northern Baffin Island. Growth rates analyzed from scanning electron microscope images and Mg/Ca cycle widths (Fig. S3); error bars show SD. The red squares are individual specimens. Satellite-derived SST data for each locality were obtained from Reynolds et al. (1). Growth rate decline is uniform from the Gulf of Maine (GOM) at 43°N northwards to 52°N (northern Newfoundland (NE NF). From that point, even though temperatures continue to decline slowly, growth declines sharply to 61 µm/y at 73°N (Arctic Bay). This results in a significant departure from the linear relationship of growth and temperature. A linear relationship not only exists for *C. compactum* south of 52°N, but was also experimentally determined for several Subarctic coralline species (2). If sea-ice cover persists for more than 2 mo, growth ceases, likely due to lack of sufficient stored photosynthate. Growth north of 52°N in the western Labrador Sea and Baffin Island region is therefore related to declining solar insolation on the seafloor due to snow-covered sea ice (marked as sea ice delta; blue line) (SE NF, southeastern Newfoundland; S. Lab, southern Labrador; N. Lab, Northern Labrador; modified from Adey et al. (3). Light attenuation of sea ice can vary according to age of ice (multi- or single-year ice), thickness, ice type, snow cover, meltwater ponds, and growth of ice-algal mats. However, even assuming thin (~1 m) single-year blue ice without snow cover and ice algae, photosynthetically active radiation (PAR)-spectrum light penetration is only about 30% (4). Considering fall and winter darkness, this results in highly limited amounts of light reaching the seafloor. By the time spring light conditions return, snow cover, white ice, and meltpond formation will have additionally reduced transparency of the sea ice. Specimens of *C. compactum* used in this study were collected between 15- and 17-m water depth, which is near the lower limit of distribution of this species (3). Hence, it can be assumed that any type of sea-ice condition will be sufficient to provide low-enough amounts of light to the seafloor to inhibit photosynthetic activity and therefore significant calcification in *C. compactum* during periods of sea-ice coverage.

1. Reynolds RW, Rayner NA, Smith TM, Stokes DC, Wang W (2002) An improved in situ and satellite SST analysis for climate. *J Clim* 15:1609–1625.
2. Adey WH (1970) The effects of light and temperature on growth rates in boreal-subarctic crustose corallines. *J Phycol* 6:269–276.
3. Adey WH, Halfar J, Williams B (2013) The coralline genus *Clathromorphum* Foslie emend. Adey: Biological, physiological, and ecological factors controlling carbonate production in an Arctic-Subarctic climate archive. *Smithsonian Contributions to the Marine Sciences* (Smithsonian Institution Scholarly Press, Washington, DC), Vol 40, pp 1–48.
4. Maykut GA, Grenfell TC (1975) The spectral distribution of light beneath first-year sea ice in the Arctic Ocean. *Limnol Oceanogr* 20(4):554–563.

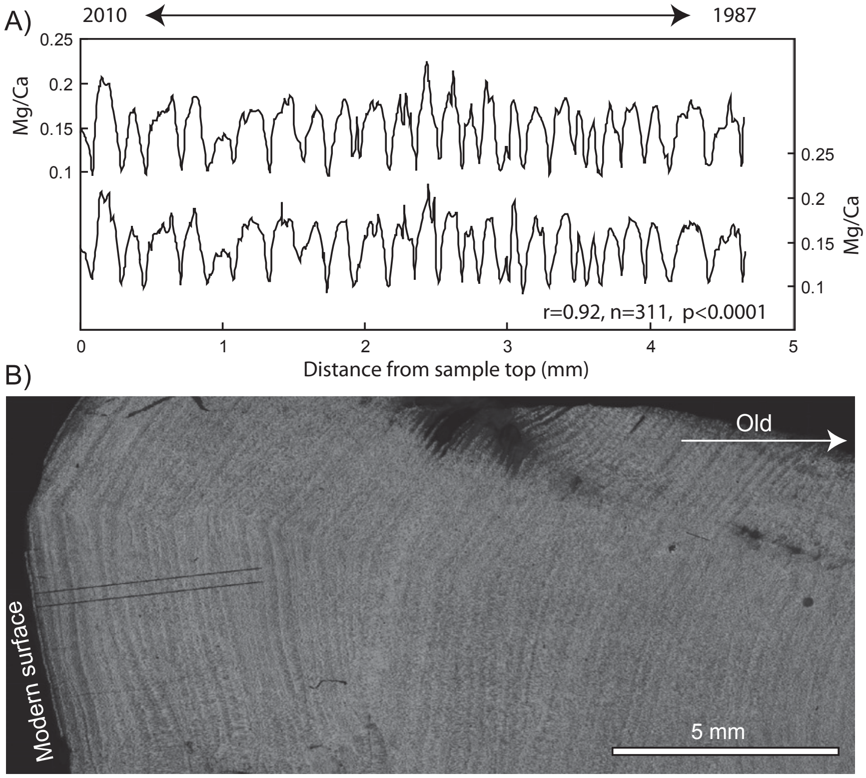

Fig. S2. Analytical reproducibility. Annual cycles of Mg/Ca ratios measured by electron microprobe (*A*) on two parallel transects along main axis of growth on uppermost 5 mm of sample Ki2 (*B*). Microscope image of polished sample shows ~80 annual growth increments. Cycle shapes in *A* are characteristic of break in growth during sea-ice season, with narrow downward pointing peak. Summer portions of cycles instead are smooth, reflecting summer light and temperature cycle patterns following spring breakup of sea ice. Note similarity of winter Mg/Ca ratios reflecting constant seawater temperature under sea ice. Sample spacing, 15 μm (average annual growth of Ki2 = 172 μm) results in average resolution of ~11.5 samples per year. Mg/Ca ratios are based on atom percent of Mg and Ca.

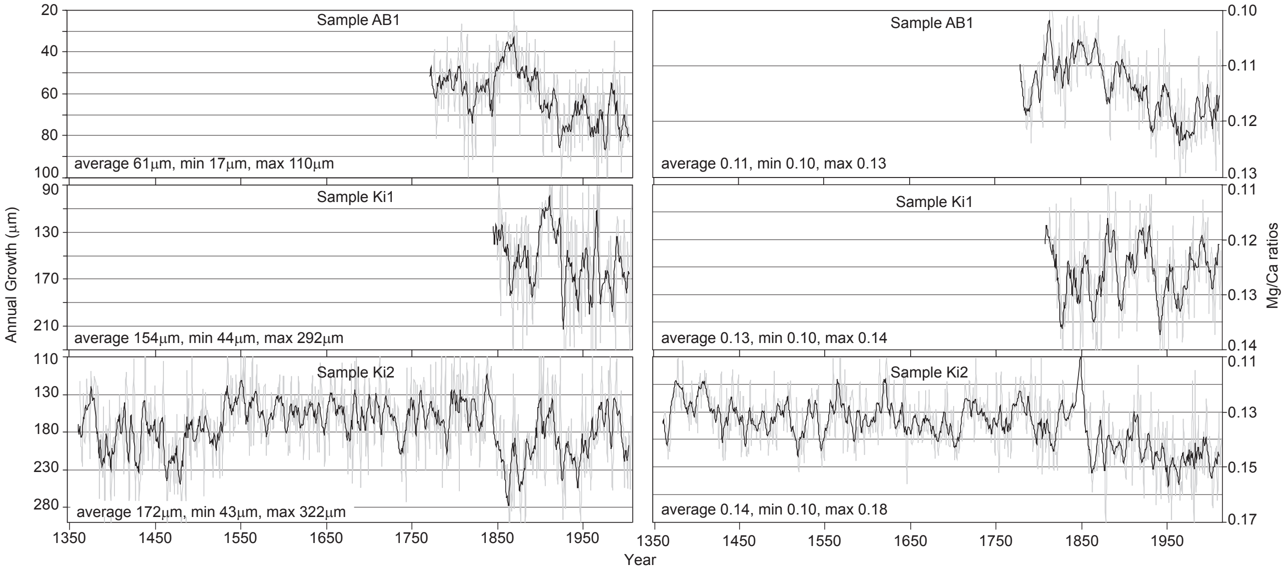

Fig. S3. Annual growth and Mg/Ca ratios of individual samples. Gray lines show annual data, black lines indicate five-point moving average. Note that in accordance with Fig. 3, *y* axes values are plotted in reverse order. A common trend toward increasing growth and higher Mg/Ca ratios (= less sea-ice) is apparent from the mid-19th century onwards. Using the individual records shown here, a combined algal growth increment width and Mg/Ca ratio time series was calculated by averaging equally weighted normalized time series (Fig. 3). Combining multiple proxy records from various locations reduces local and sample-specific variability as has been demonstrated before for coralline algae (1).

1. Halfar J, et al. (2011) Coralline algal growth-increment widths archive North Atlantic climate variability. *Palaeogeogr Palaeoclimatol Palaeoecol* 302:71–80.

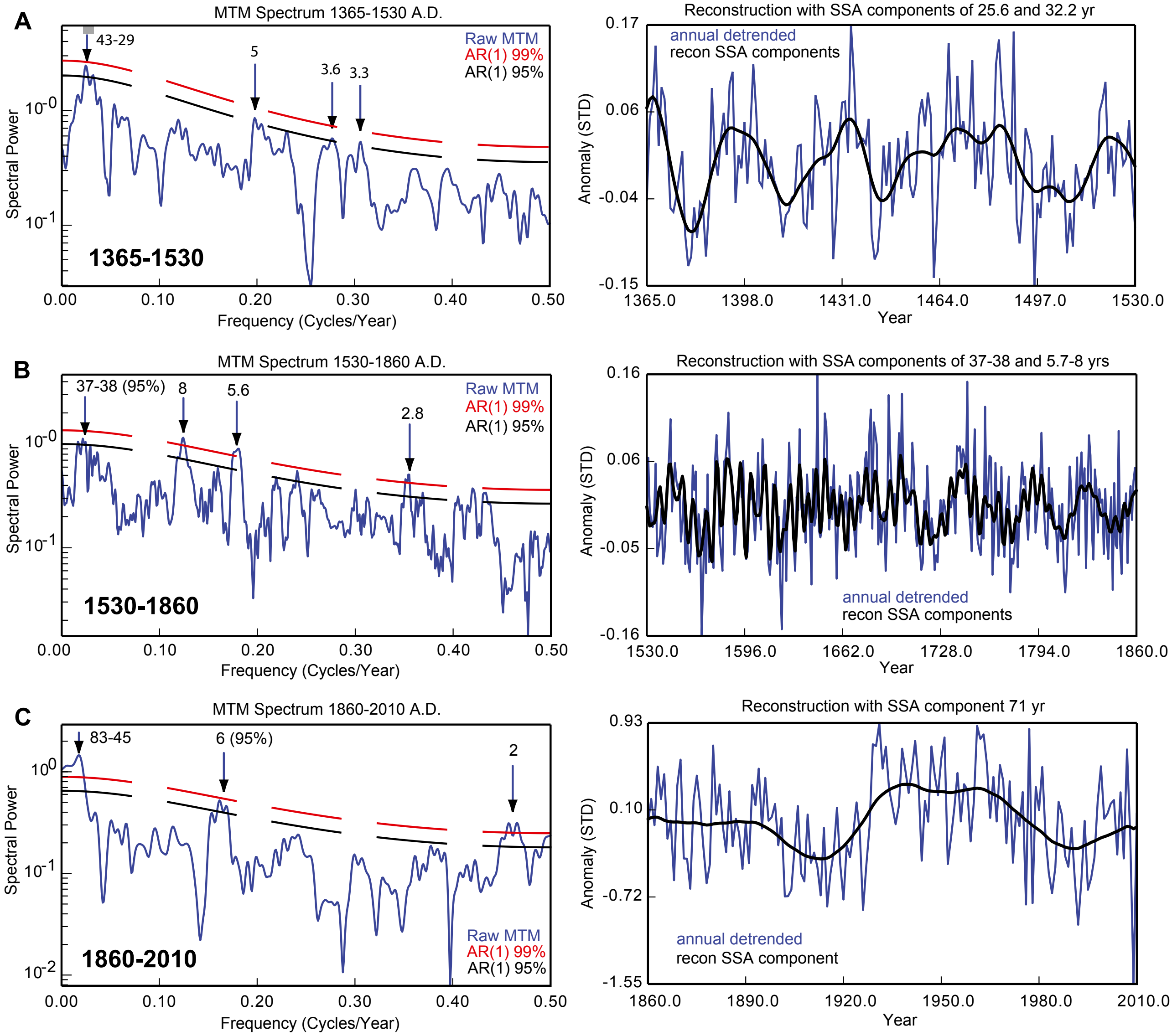

Fig. S4. Spectral analysis of annually averaged algal time series for (*A*) 1365–1530, (*B*) 1530–1860, and (*C*) 1860–2010 time intervals. Periods (years) of peaks significant at the 95/99% level are indicated (multitaper method, MTM, *Left*). The significance estimates in the MTM are independent of the spectral power. (*Right*) Annual detrended algal time series (blue) and dominant reconstructed singular spectrum analysis (SSA) components (black). For spectral analysis of coralline algal data the SSA–MTM Toolkit (1) was used. Before spectral analysis, time series were normalized to unit variance and detrended by removing the linear trend. The MTM (*Left*) was applied, which provides useful tools for spectral estimation (1) and signal reconstruction with high spectral resolution and significance tests. The significance tests are independent of the spectral power, therefore even oscillations with small amplitudes can be identified with a high significance level in a time series whose spectrum may contain both broadband and line components (1). Using the MTM, a small set of data tapers, or data windows, is applied to the data in the time domain to reduce the variance of spectral estimates before Fourier transformation (2). This method has been widely used for problems in geophysical signal analysis, for example analyses of instrumental data of the atmosphere and ocean, and paleoclimate proxy data (2, 3). A detailed description of this method can be found in Ghil et al. (1).

1. Ghil M, et al. (2002) Advanced spectral methods for climatic time series. *Rev Geophys* 40(1):1–41.
2. Thompson DJ (1982) Spectrum estimation and harmonic analysis. Institute of Electrical and Electronics Engineers Proceedings (Institute of Electrical and Electronics Engineers, Washington, DC), 70(1055–1096).
3. Mann ME, Lees J (1996) Robust estimation of background noise and signal detection in climatic time series. *Clim Change* 33:409–445.

Table S1. Results from AMS radiocarbon dating of sample Ki2

Sample	Measured age, B.P.	$^{13}C/^{12}C$, ‰	Conventional age, B.P.	2σ calibration	Expected*
RC1	140 ± 30	−2.0	520 ± 30	Cal AD 1820–post-1950	1875–1880
RC2	240 ± 30	+0.5	660 ± 30	Cal AD 1670–1840	1815–1825
RC3	670 ± 30	0.0	1080 ± 30	Cal AD 1310–1440	1435–1445

Samples were measured by Beta Analytics, Inc. Expected, age determined by age model based on growth increments and Mg/Ca cycles (Fig. S2). RC, radiocarbon sample; Cal AD, calibrated anno domini.

*Age determined.